ARTICLE

https://doi.org/10.1038/s41586-018-0042-1

Quaternary stereocentres via an enantioconvergent catalytic S_N1 reaction

Alison E. Wendlandt[1], Prithvi Vangal[1] & Eric N. Jacobsen[1]*

The unimolecular nucleophilic substitution (S_N1) mechanism features prominently in every introductory organic chemistry course. In principle, stepwise displacement of a leaving group by a nucleophile via a carbocationic intermediate enables the construction of highly congested carbon centres. However, the intrinsic instability and high reactivity of the carbocationic intermediates make it very difficult to control product distributions and stereoselectivity in reactions that proceed via S_N1 pathways. Here we report asymmetric catalysis of an S_N1-type reaction mechanism that results in the enantioselective construction of quaternary stereocentres from racemic precursors. The transformation relies on the synergistic action of a chiral hydrogen-bond-donor catalyst with a strong Lewis-acid promoter to mediate the formation of tertiary carbocationic intermediates at low temperature and to achieve high levels of control over reaction enantioselectivity and product distribution. This work provides a foundation for the enantioconvergent synthesis of other fully substituted carbon stereocentres.

Quaternary stereogenic centres are important structural motifs in natural products and biologically active compounds, conferring valuable structural, conformational and metabolic properties. Their construction has long been recognized as an important challenge to the field of chemical synthesis, and several distinct catalytic, enantioselective approaches have been developed in response[1–4]. Notable examples include cycloadditions[5], α- and β-alkylation and arylation of carbonyls[6–8], 3,3′-additions[9], S_N2' reactions[10] and Heck-type

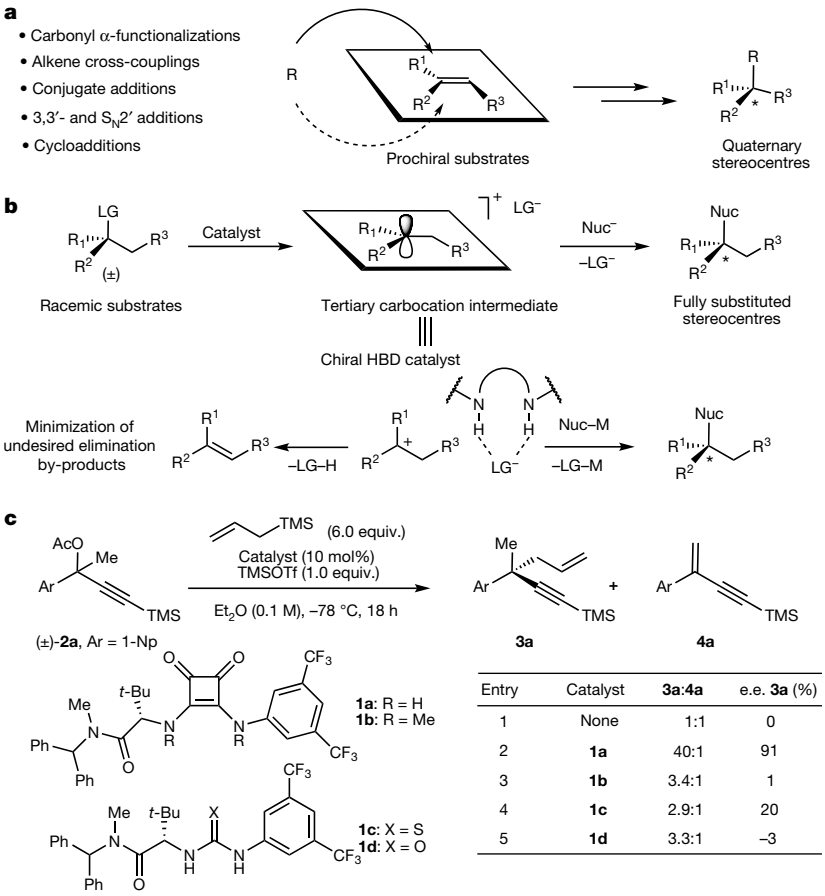

Entry	Catalyst	3a:4a	e.e. 3a (%)
1	None	1:1	0
2	**1a**	40:1	91
3	**1b**	3.4:1	1
4	**1c**	2.9:1	20
5	**1d**	3.3:1	–3

Fig. 1 | Approaches to the enantiocontrolled construction of quaternary stereocentres. **a**, Traditional methods for the synthesis of quaternary-stereocentre-containing molecules use stereochemically defined prochiral substrates. **b**, The S_N1 approach to the construction of quaternary stereocentres described here. **c**, Enantioselective allylation of propargyl acetates using chiral squaramide catalysts and TMSOTf as a promoter. LG, leaving group; Np, naphthyl; TMS, trimethylsilyl.

[1]Department of Chemistry and Chemical Biology, Harvard University, Cambridge, MA, USA. *e-mail: jacobsen@chemistry.harvard.edu

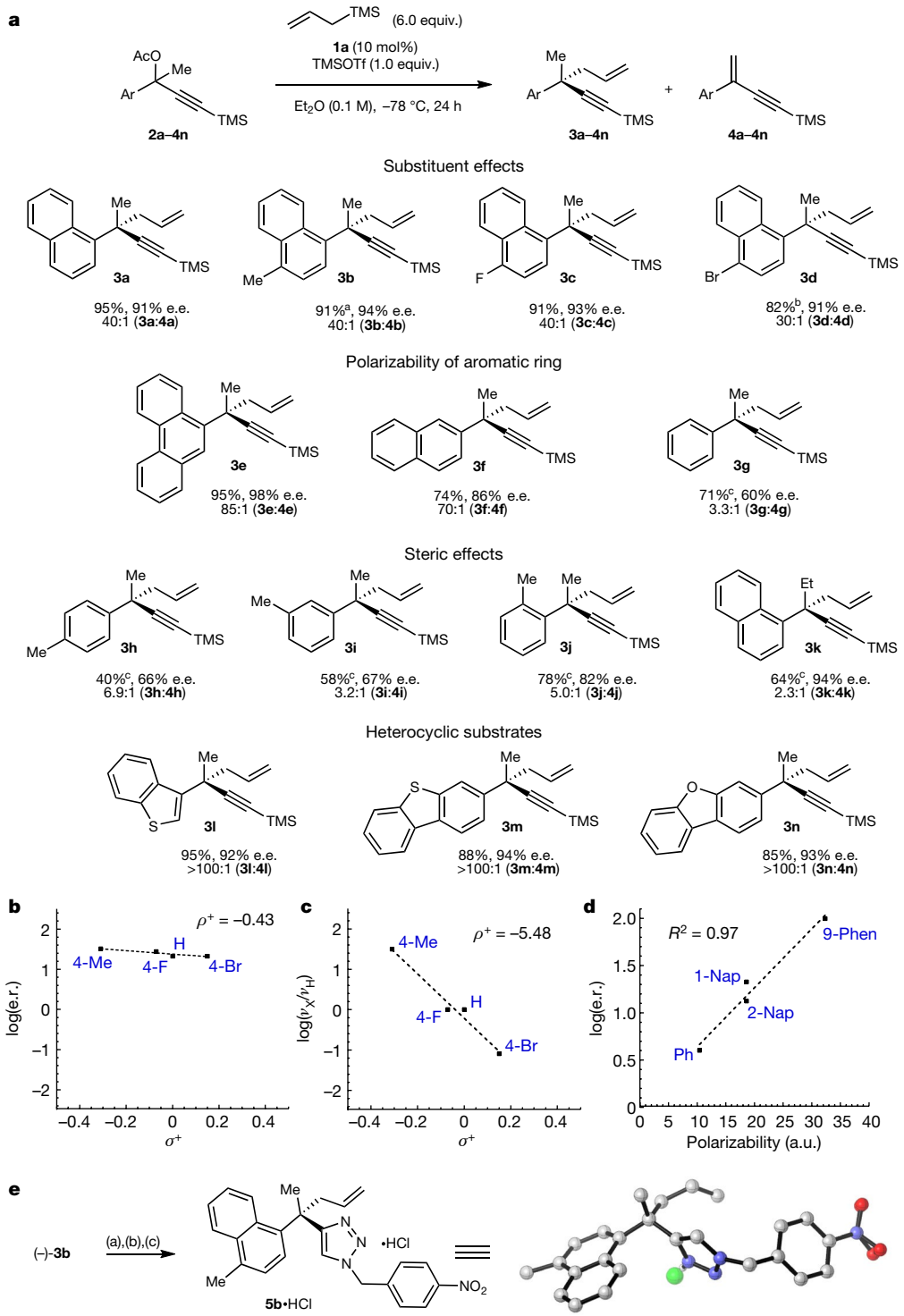

Fig. 2 | Asymmetric allylation of propargyl acetates. a, Substrate scope. Reactions were run on a 0.6-mmol scale with 0.1 equiv. **1a**, 1.0 equiv. TMSOTf and 6.0 equiv. allyltrimethylsilane in 0.1 M Et_2O at −78 °C for 24 h. [a]Reaction time was 4 h. [b]Reaction time was 14 d. [c]NMR yield. **b**, **c**, Hammett plot of the σ^+ values of the substituents in **2a**–**2d** versus the enantiomeric ratios (log(e.r.)) obtained in the formation of **3a**–**3d** (**b**) ($\rho^+ = -0.43$) and versus the relative reaction rates ($\log(\nu_X/\nu_H)$) determined for each substrate (**c**) ($\rho^+ = -5.48$). **d**, Linear free-energy plot of the calculated polarizability of the aromatic rings in **2a** and **2e**–**2 g** versus the enantiomeric ratios (log(e.r.)) obtained in the formation of **3a** and **3e**–**3g** ($R^2 = 0.97$). a.u., arbitrary units. **e**, The absolute configuration of (−)-**3b** was determined by X-ray crystallography (structure shown), following derivatization to triazole **5b**; the configuration of all other products was assigned by analogy. Conditions: (a) tetra-*n*-butylammonium fluoride (2.0 equiv.), THF, room temperature; (b) 4-nitrobenzylbromide (1.1 equiv.), NaN_3 (1.1 equiv.), $CuSO_4$ (0.1 equiv.), sodium ascorbate (0.2 equiv.), *t*BuOH/H_2O (1:2), 50 °C; (c) HCl (3 M in Et_2O).

cross-couplings[11]. Each of these methods relies on enantiofacial addition across a prochiral substrate (Fig. 1a) and therefore requires the preparation of stereochemically well-defined starting materials (such as trisubstituted olefins) and subsequent enantioselective bond formation.

We envisioned that stepwise nucleophilic substitution reactions that proceed through prochiral carbocationic intermediates could provide a useful and complementary strategy for the enantioselective synthesis of compounds with quaternary stereocentres. Unlike the synthetic approaches noted above, quaternary-stereocentre construction via an S_N1-like pathway might be stereoablative[12] and could therefore use readily accessed racemic compounds as substrates (Fig. 1b). Although realization of this strategy would lift the requirement for stereocontrol in the synthesis of the substrate, doing so requires several very substantial challenges to be overcome. The requisite catalytic system must (a) generate a reactive tertiary carbocationic intermediate, (b) minimize undesired elimination and rearrangement pathways, and (c) exert enantiocontrol in additions of a carbon-centred nucleophile to a high-energy cationic intermediate. As a result, despite the practical appeal of an enantioconvergent approach to the construction of quaternary stereocentres, only isolated examples have been reported so far[9,13,14].

Over the past decade, chiral, dual hydrogen-bond-donor (HBD) catalysts have been developed that promote enantioselective nucleophilic substitution and addition reactions via ion-pair intermediates. These catalysts promote ion-pair formation via direct anion abstraction[15] or by substrate protonation with a co-catalytic Brønsted acid[16].

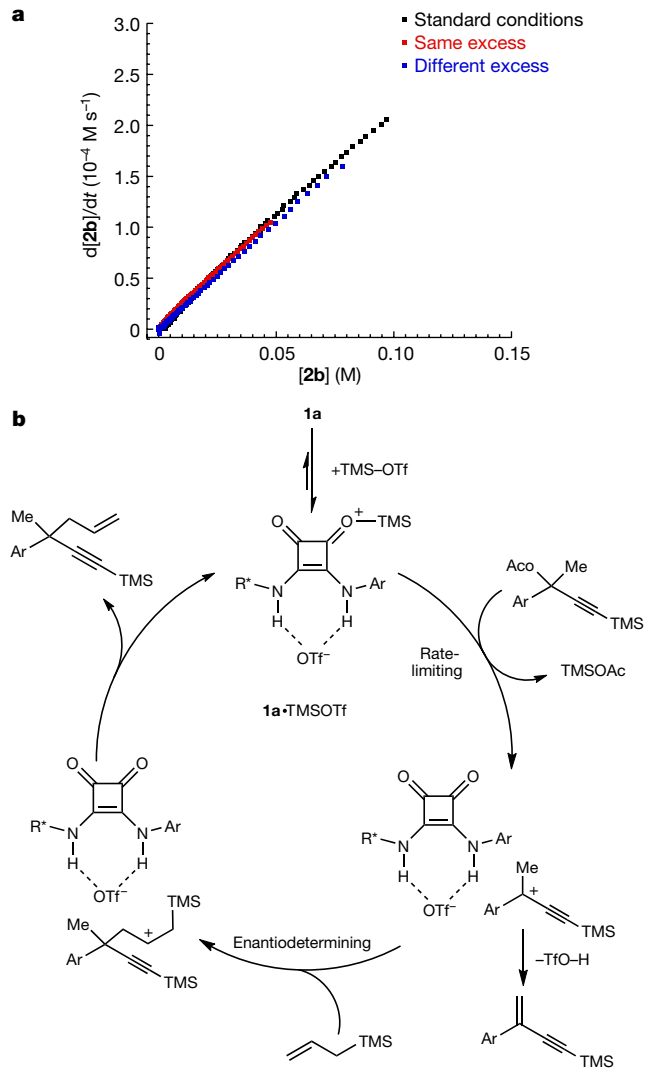

Fig. 3 | Kinetic data and catalytic cycle. a, Reaction-progress kinetic analysis of the reaction of **2b** with allyltrimethylsilane ([**2b**], concentration of **2b**). Standard conditions: $[\text{allyltrimethylsilane}]_0 = 0.25$ M, $[\mathbf{2b}]_0 = 0.10$ M; 'same excess' conditions: $[\text{allyltrimethylsilane}]_0 = 0.195$ M, $[\mathbf{2b}]_0 = 0.047$ M; 'different excess' conditions: $[\text{allyltrimethylsilane}]_0 = 0.315$ M, $[\mathbf{2b}]_0 = 0.08$ M; $[X]_0$, initial concentration of X. **b**, Proposed catalytic mechanism for the enantioselective allylation of propargyl acetates.

Asymmetric induction is typically achieved from the resultant ion pair as a consequence of specific attractive non-covalent interactions between the corresponding cationic intermediate and the chiral HBD catalyst[17–19]. Reported examples have been limited to heteroatom-stabilized cations, owing to the challenges in generating the requisite ion pair and suppressing elimination and rearrangement pathways. The ability of HBD catalysts to control enantioselective nucleophile addition into non-heteroatom-stabilized carbocations has, to our knowledge, not been demonstrated.

It was discovered recently that chiral squaramide catalysts could be used in conjunction with Lewis acids such as trimethylsilyl trifluoromethanesulfonate (TMSOTf) to promote enantioselective reactions[20]. This dual-catalyst system was shown to promote the formation of oxocarbenium ions from dialkyl acetals—substrates that are unreactive under previously developed HBD-promoted reaction manifolds—while still engaging in attractive non-covalent interactions to achieve enantioinduction. We envisioned that the strong ionizing ability of this dual-catalyst system could provide access to carbocationic intermediates that lack heteroatom stabilization, thus allowing us to examine whether small-molecule HBDs can be used to promote productive, enantioselective reaction pathways from such high-energy intermediates.

Reaction development

After an extensive evaluation of potential tertiary electrophile–carbon-centred nucleophile coupling partners, the reaction of propargyl acetate **2a** with allyltrimethylsilane was identified as a useful model system with which to test this proposal (Fig. 1c). In the absence of an HBD catalyst, the Lewis-acid-promoted reaction affords a 1:1 mixture of the desired product **3a** and the elimination product **4a** (Fig. 1c, entry 1). When readily accessed squaramide **1a** (10 mol%) was added to the reaction, however, **3a** was obtained in high yield (40:1 **3a**:**4a**; Fig. 1c, entry 2) and enantioselectivity (91% enantiomeric excess, e.e.). Product ratio and enantioselectivity were strongly dependent on the nature of the HBD moiety: the related *N*,*N*-dimethylated squaramide (**1b**), thiourea (**1c**) and urea (**1d**) catalysts afforded **3a** in low yield and enantiomeric excess (Fig. 1c, entries 3–5). No reaction was observed with squaramide, thiourea or urea HBD catalysts in the absence of TMSOTf.

We then evaluated a series of tertiary propargyl acetates to probe the reaction scope and to generate preliminary information about the mechanism of the enantioselective substitution reaction (Fig. 2a). Substrates with electron-donating (such as **2b** and **2c**) and electron-withdrawing (**2d**) substituents underwent allylation with high enantioselectivity (>90% e.e.) and product selectivity (>30:1 **3**:**4**). A linear correlation with a small negative slope ($\rho^+ = -0.43$, Fig. 2b) was observed between the Hammett substituent σ^+ constants and log(e.r.) for substrates **2a**–**2d** (e.r., enantiomeric ratio). By contrast, a linear correlation with a large negative slope ($\rho^+ = -5.48$, Fig. 2c) was obtained from the corresponding plot of the σ^+ constants versus $\log(\nu_X/\nu_H)$ for the same substrates (where ν_X/ν_H is the reaction rate of substrate that contains substituent X relative to that of the analogous unsubstituted substrate). The observation of a linear free-energy dependence (ρ^+) of this magnitude provides direct evidence of positive charge accumulation in the rate-determining transition state, consistent with an S_N1-type ionization mechanism[21].

Despite the very subtle dependence of enantiomeric excess on the electronic properties of the substrate substituents noted above, reaction enantioselectivity was strongly responsive to changes in the expanse and position of the aryl moiety of the substrate. A linear correlation was observed between polarizability values calculated for the aryl substituent[22] and log(e.r.) of products **3a** and **3e**–**3g** (Fig. 2d), indicating that stabilizing aromatic interactions are likely to serve as a contributing factor in enantiodifferentiation[23]. Evidence for the existence of such stabilizing interactions could be gleaned from computational analysis of the putative complex between catalyst **1a** and substrate **2a** (Supplementary Fig. 9). Steric congestion near the reaction site also correlates with enantioselectivity. Thus, the *o*-tolyl-substituted derivative **2j** underwent an allylation reaction to afford a product with higher enantiomeric excess (82%) than obtained using the *p*- or *m*-substituted analogues **2h** and **2i** (66%–67%). Similarly, the ethyl-substituted product **3k** was obtained in higher enantiomeric excess (94%) than the methyl-substituted product **3b** (91%).

Substrates containing electron-rich heterocycles also underwent highly enantioselective substitution. Representative S- and O-heterocyclic substrates underwent reaction with allyltrimethylsilane to afford quaternary products (**3l**–**3n**) in high yield and enantiomeric excess and with no detectable elimination by-products. Following derivatization, the absolute stereochemistry of product **3b** was determined by using X-ray crystallography (Fig. 2e).

Mechanistic studies

We undertook a mechanistic study of the reaction between a representative tertiary propargyl acetate substrate and allyltrimethylsilane promoted by squaramide **1a** and TMSOTf to obtain insights into the underlying catalytic mechanism. The disappearance of **2b** could be monitored over the entire course of the reaction using in situ infrared

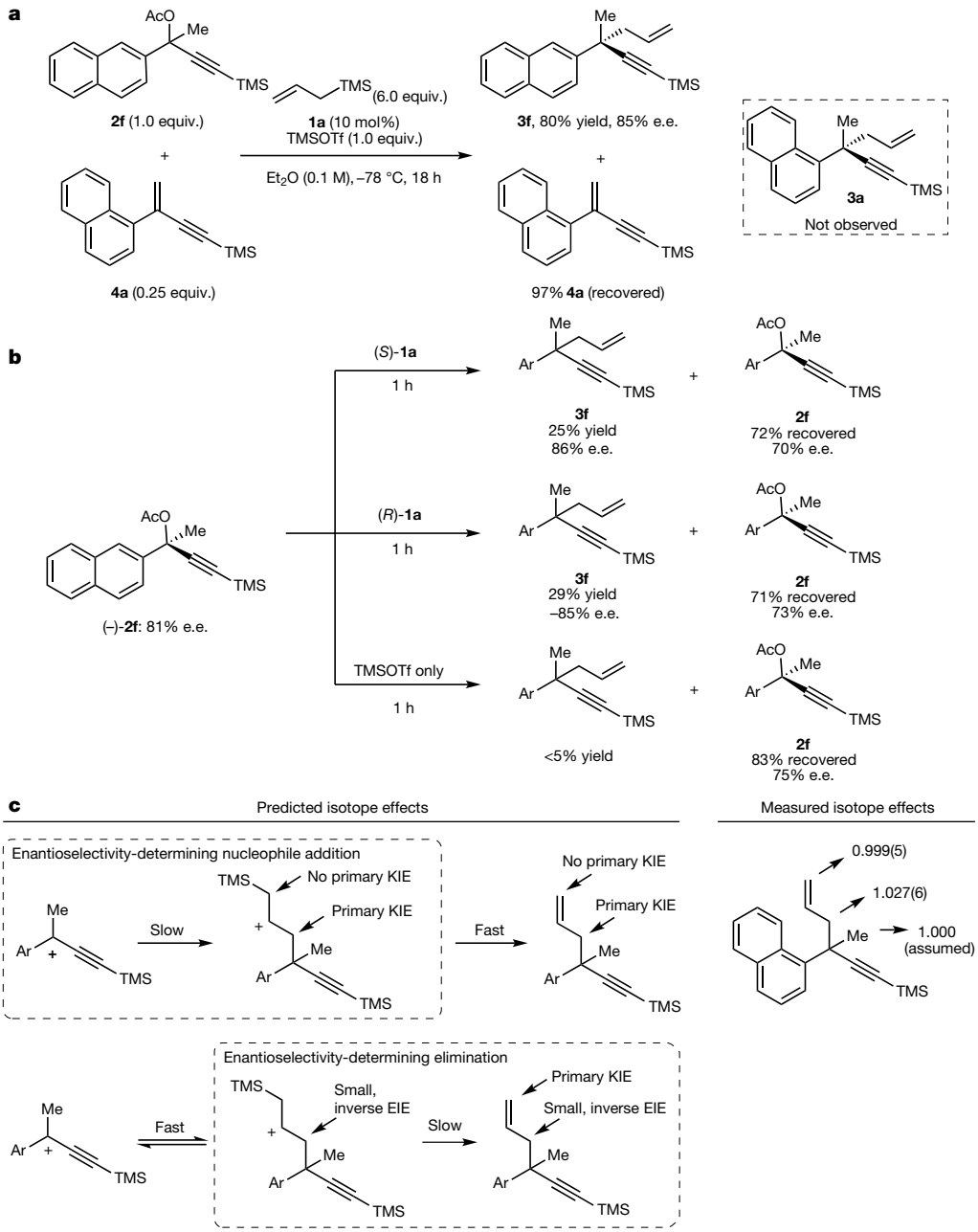

Fig. 4 | Mechanistic studies to probe the post-rate-limiting steps of the allylation reaction. **a**, Crossover experiment to establish the irreversible formation of the alkene by-product (illustrated here for **4a**). **b**, Partial reaction with scalemic **2f**, demonstrating that allylation proceeds via a stereoablative mechanism rather than by a dynamic kinetic-Resolution process. **c**, Predicted and measured $^{12}C/^{13}C$ kinetic isotope effects (KIEs) and equilibrium isotope effects (EIEs). The experimentally determined isotope effects (numbers) are consistent with the predicted mechanistic scenario (top row).

spectroscopy. Runs carried out at different initial concentrations of **2b** but with the same excess in concentration of allyltrimethyl silane (a 'same-excess' experiment[24]) produce good graphical overlay in the kinetic data (Fig. 3a), demonstrating that no catalyst decomposition or product inhibition occurs over the course of the reactions. The linearity of the plot further indicates that the reaction obeys a first-order rate dependence overall. Runs carried out with a different excess in the initial concentration of allyltrimethyl silane relative to **2b** also produce good overlay in the kinetic data (a 'different-excess' experiment[24]), revealing that the reaction obeys a first-order rate dependence on the concentration of **2b** and has no rate dependence on the concentration of allyltrimethylsilane. These kinetic findings are consistent with a stepwise reaction mechanism whereby substrate C–O cleavage is turnover-limiting and nucleophile addition occurs in a post-turnover-limiting step (Fig. 3b). Kinetic studies further revealed a sub-first-order dependence of the reaction rate on the concentration of TMSOTf, and a first-order dependence of the reaction rate on the concentration of **1a** with a non-zero *y* intercept. The kinetic dependence on the concentrations of **1a** and TMSOTf is consistent with pre-equilibrium formation of a resting-state **1a**·TMSOTf complex that reacts directly with substrate **2**. The non-zero *y* intercept is consistent with the competing background reaction that is observed in the absence of **1a** (see Supplementary Information). The observation that optimal enantioselectivities are obtained under conditions where a background, uncatalysed reaction is expected is intriguing, and the subject of continued study.

Having established that the squaramide-TMSOTf-promoted formation of the carbocationic intermediate is rate-limiting, we performed a series of experiments to interrogate the critical post-rate-limiting steps. We determined that the formation of the elimination by-product was irreversible on the basis of a crossover experiment in which 1-naphthyl-substituted enyne (**4a**, 0.25 equiv.) was introduced to the reaction of 2-naphthyl-substituted acetate (**2f**) under otherwise standard reaction conditions. This reaction afforded 2-naphthyl-substituted product **3f** in 80% yield, and alkene **4a** was recovered in 97% yield with no trace of 1-naphthyl allylated product **3a** detected (Fig. 4a).

To evaluate whether the reaction proceeds through an enantioselective or enantiospecific mechanism, the allylation was carried out by subjecting scalemic substrate (−)-**2f** (81% e.e.) to both enantiomers of the squaramide catalyst **1a** (Fig. 4b). After 1 h of reaction time,

product **3f** was obtained in 86% enantiomeric excess and 24% yield using (*S*)-**1a**; in the presence of (*R*)-**1a**, product **3f** was obtained in similar yield but with opposite enantioselectivity (−85% e.e.). In both cases, the substrate **2f** that was recovered was observed to have undergone only a small degree of epimerization, comparable to that observed when **2f** was treated with TMSOTf and in the absence of squaramide catalyst. The results of these experiments are consistent with a stereoablative mechanism, that is, an enantioselective process that proceeds through an achiral carbocationic intermediate. By contrast, a dynamic kinetic-Resolution pathway can be ruled out, whereby **2f** undergoes rapid racemization and one enantiomer preferentially undergoes stereospecific substitution.

We considered two limiting mechanistic possibilities with regard to the enantiodetermining step: (a) irreversible nucleophile addition followed by rapid silyl elimination (Fig. 4c, top), and (b) rapid and reversible nucleophile addition, followed by enantiodetermining silyl elimination (Fig. 4c, bottom). These two scenarios are predicted to produce different carbon isotope effects at the allyl fragment. The carbon kinetic isotope effects (KIEs) were determined with natural-abundance materials using an NMR methodology[25] (Fig. 4c, see Supplementary Information). A large primary KIE of 1.027 was observed at the position of bond formation (internal allylic methylene), whereas no KIE was observed at the terminal position. These results demonstrate that the first C–C bond-forming step is irreversible and therefore enantiodetermining.

Conclusion

We have shown that the cooperative effect of chiral squaramides and TMSOTf generates tertiary carbocations that lack heteroatom stabilization from racemic precursors, controls enantioselectivity in additions of a carbon-centred nucleophile, and attenuates undesired elimination pathways. The strategy outlined here may be generalizable to the construction of many types of highly congested stereogenic centre.

Data availability

The crystallographic data for compound **5b**·HCl can be obtained free of charge from the Cambridge Crystallographic Data Centre (https://www.ccdc.cam.ac.uk) under identifier CCDC 1822228. The raw data for the kinetics experiments are available from the corresponding author on request. All other data that support these findings are available within the paper or Supplementary Information.

Received: 8 November 2017; Accepted: 23 February 2018;
Published online 25 April 2018.

1. Quasdorf, K. W. & Overman, L. E. Catalytic enantioselective synthesis of quaternary carbon stereocentres. *Nature* **516**, 181–191 (2014).
2. Liu, Y., Han, S.-J., Liu, W.-B. & Stoltz, B. M. Catalytic enantioselective construction of quaternary stereocenters: assembly of key building blocks for the synthesis of biologically active molecules. *Acc. Chem. Res.* **48**, 740–751 (2015).
3. Das, J. P. & Marek, I. Enantioselective synthesis of all-carbon quaternary stereogenic centers in acyclic systems. *Chem. Commun.* **47**, 4593–4623 (2011).
4. Feng, J., Holmes, M. & Krische, M. J. Acyclic quaternary carbon stereocenters via enantioselective transition metal catalysis. *Chem. Rev.* **117**, 12564–12580 (2017).
5. Wilson, R. M., Jen, W. S. & MacMillan, D. W. C. Enantioselective organocatalytic intramolecular Diels–Alder reactions. The asymmetric synthesis of solanapyrone D. *J. Am. Chem. Soc.* **127**, 11616–11617 (2005).
6. Krautwald, S., Sarlah, D., Schafroth, M. A. & Carreira, E. M. Enantio- and diastereo-divergent dual catalysis: α-allylation of branched aldehydes. *Science* **340**, 1065–1068 (2013).
7. Behenna, D. C. & Stoltz, B. M. The enantioselective Tsuji allylation. *J. Am. Chem. Soc.* **126**, 15044–15045 (2004).
8. Murphy, J. J., Bastida, D., Paria, S., Fagnoni, M. & Melchiorre, P. Asymmetric catalytic formation of quaternary carbons by iminium ion trapping of radicals. *Nature* **532**, 218–222 (2016).
9. Zhang, P., Le, H., Kyne, R. E. & Morken, J. P. Enantioselective construction of all-carbon quaternary centers by branch-selective Pd-catalyzed allyl–allyl cross-coupling. *J. Am. Chem. Soc.* **133**, 9716–9719 (2011).
10. Jung, B. & Hoveyda, A. H. Site- and enantioselective formation of allene-bearing tertiary or quaternary carbon stereogenic centers through NHC–Cu-catalyzed allylic substitution. *J. Am. Chem. Soc.* **134**, 1490–1493 (2012).
11. Mei, T.-S., Patel, H. H. & Sigman, M. S. Enantioselective construction of remote quaternary stereocentres. *Nature* **508**, 340–344 (2014).
12. Bhat, V., Welin, E. R., Guo, X. & Stoltz, B. M. Advances in stereoconvergent catalysis from 2005 to 2015: transition-metal-mediated stereoablative reactions, dynamic kinetic Resolutions, and dynamic kinetic asymmetric transformations. *Chem. Rev.* **117**, 4528–4561 (2017).
13. Braun, M. & Kotter, W. Titanium(IV)-catalyzed dynamic kinetic asymmetric transformation of alcohols, silyl ethers, and acetals under carbon allylation. *Angew. Chem. Int. Ed.* **43**, 514–517 (2004).
14. Zhao, W., Wang, Z., Chu, B. & Sun, J. Enantioselective formation of all-carbon quaternary stereocenters from indoles and tertiary alcohols bearing a directing group. *Angew. Chem. Int. Ed.* **54**, 1910–1913 (2015).
15. Reisman, S. E., Doyle, A. G. & Jacobsen, E. N. Enantioselective thiourea-catalyzed additions to oxocarbenium ions. *J. Am. Chem. Soc.* **130**, 7198–7199 (2008).
16. Xu, H., Zuend, S. J., Woll, M. G., Tao, Y. & Jacobsen, E. N. Asymmetric cooperative catalysis of strong Brønsted acid-promoted reactions using chiral ureas. *Science* **327**, 986–990 (2010).
17. Brak, K. & Jacobsen, E. N. Asymmetric ion-pairing catalysis. *Angew. Chem. Int. Ed.* **52**, 534–561 (2013).
18. Kennedy, C. R., Lin, S. & Jacobsen, E. N. The cation–π interaction in small-molecule catalysis. *Angew. Chem. Int. Ed.* **55**, 12596–12624 (2016).
19. Neel, A. J., Hilton, M. J., Sigman, M. S. & Toste, F. D. Exploiting non-covalent π interactions for catalyst design. *Nature* **543**, 637–646 (2017).
20. Banik, S. M., Levina, A., Hyde, A. M. & Jacobsen, E. N. Lewis acid enhancement by hydrogen-bond donors for asymmetric catalysis. *Science* **358**, 761–764 (2017).
21. Brown, H. C. & Okamoto, Y. Substituent constants for aromatic substitution. *J. Am. Chem. Soc.* **79**, 1913–1917 (1957).
22. McKinney, J. D., Gottschalk, K. E. & Pedersen, L. The polarizability of planar aromatic systems. An application to polychlorinated biphenyls (PCB's), dioxins and polyaromatic hydrocarbons. *J. Mol. Struct. (Theochem)* **105**, 427–438 (1983).
23. Hunter, C. A. & Sanders, J. K. M. The nature of π–π interactions. *J. Am. Chem. Soc.* **112**, 5525–5534 (1990).
24. Blackmond, D. G. Reaction progress kinetic analysis: a powerful methodology for mechanistic studies of complex catalytic reactions. *Angew. Chem. Int. Ed.* **44**, 4302–4320 (2005).
25. Singleton, D. A. & Thomas, A. A. High-precision simultaneous determination of multiple small kinetic isotope effects at natural abundance. *J. Am. Chem. Soc.* **117**, 9357–9358 (1995).

Acknowledgements Financial support for this work was provided by the NIH through GM043214 and a postdoctoral fellowship to A.E.W. We thank S. McCann and C. Fry for assistance with NMR experiments, E. E. Kwan for discussions regarding the KIE studies, and S.-L. Zheng for X-ray structure determination.

Reviewer information *Nature* thanks R. Gilmour and the other anonymous reviewer(s) for their contribution to the peer review of this work.

Author contributions A.E.W. and E.N.J. conceived the work, A.E.W. and P.V. conducted the experiments, E.N.J. directed the research, and A.E.W., P.V. and E.N.J. wrote the manuscript.

Competing interests The authors declare no competing interests.

Additional information
Supplementary information is available for this paper at https://doi.org/10.1038/s41586-018-0042-1.
Reprints and permissions information is available at http://www.nature.com/reprints.
Correspondence and requests for materials should be addressed to E.N.J.
Publisher's note: Springer Nature remains neutral with regard to jurisdictional claims in published maps and institutional affiliations.